2012 IEEE International Conference on Robotics and Automation
RiverCentre, Saint Paul, Minnesota, USA
May 14-18, 2012

Stable Dynamic Walking of the Quadruped "Kotetsu" Using Phase Modulations Based on Leg Loading/Unloading against Lateral Perturbations

Christophe Maufroy, Hiroshi Kimura and Tomohiro Nishikawa

Abstract*— We intend to show the basis of a general legged locomotion controller with the ability to integrate both posture and rhythmic motion controls. We respectively used leg loading and unloading for the phase transitions from swing-to-stance and stance-to-swing, and showed the following in our previous 3D model simulation study: (a) as a result of the phase modulations based on leg loading/unloading, rhythmic motion of each leg was achieved and leg coordination (resulting in a gait) emerged, even without explicit coordination among the leg controllers, allowing to realize dynamic walking in the low- to medium-speed range (b) but an additional ascending coordination mechanism between ipsilateral leg controllers was necessary to improve the stability. In this paper, we report on experimental results using "Kotetsu" under a lateral perturbation while walking and compare them with the results of our previous simulations. Detailed robot specifications and movies of the experiments can be seen at:** *http://robotics.mech.kit.ac.jp/kotetsu/.**

I. Introduction

Traditional methods for dynamic legged locomotion control are generally classified into Zero Moment Point (ZMP) based and limit-cycle based control. ZMP based control is effective for controlling posture of biped [1] and quadruped [2] robots. However, it is not good for medium or high-speed walking from the standpoint of energy consumption since a body with a large mass needs to be accelerated and decelerated by the actuators in every step cycle to satisfy the ZMP constraints. In contrast, motion generated by limit-cycle based control, making use of the natural dynamics of the system, has superior energy efficiency, but there exists an upper bound of the period of the walking cycle [3].

Based on limit-cycle based approach, dynamic walking on irregular terrain was realized with a series of quadruped robots "Tekken" [4], [5] using a neural controller made of a Central Pattern Generator [6] (CPG) and a set of reflexes. However, dynamic walk with a long cyclic period could not be realized because increasing the period caused large rolling motion of the body, leading to instabilities of walking.

Usual quadrupeds have long and narrow bodies and contralateral legs are never simultaneously in the swing phase during walking. Therefore, posture in the sagittal plane is easy to stabilize, and the main issue is to control the posture in the frontal plane, that is, to stabilize the rolling motion of the body.

This work has been partially supported by a Grant-in-Aid for Scientific Research on Priority Areas "Mobiligence" from MEXT in Japan.

C. Maufroy is with Univ. of Jena, Germany. H. Kimura and T. Nishikawa are with Kyoto Institute of Technology, Japan. christophe.maufroy@uni-jena.de, kimura61@kit.ac.jp

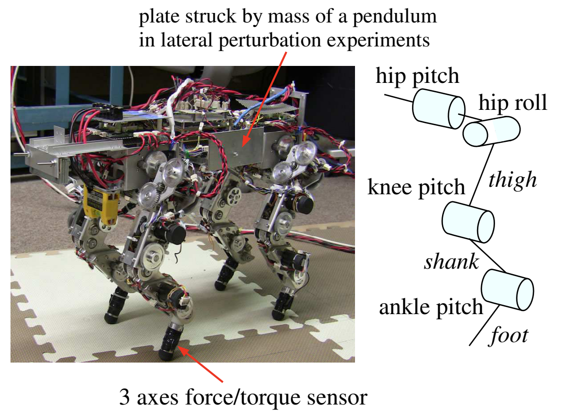

whole size	length: 34, width: 19∼25, height: 35 (cm)
mass	5.2 (kg)
DC motors	hip, knee, ankle pitch:20, hip roll:11 (W)
sensors	encoder, rate gyro (pitch&roll), 3 axes accelerometer 3 axes (force: 1 axis, torque: 2 axes) sensor

Fig. 1. Kotetsu. Top: photo and joint configuration. Bottom: specifications.

In our previous study [7] being motivated by [8], we respectively used leg loading and unloading for the phase transitions from swing-to-stance and stance-to-swing, and showed the following in 3D model simulations:

- As a result of the phase modulations based on leg unloading, rhythmic motion of each leg is achieved and leg coordination (gait) emerges, even without explicit interleg coordinations, allowing to realize dynamic walking in the low- to medium-speed range.
- The above described method has posture control ability against lateral perturbations to some extent. But an additional ascending coordination mechanism between ipsilateral legs is necessary to withstand perturbations preventing alternation of leg loading between contralateral legs.

In addition, we reported the result of first experiments of gait generation using the quadruped robot "Kotetsu" [9]. In this paper, we report on experimental results using Kotetsu under a lateral perturbation while walking, and compare them with our previous simulation results.

II. Quadruped Robot

The quadruped robot "Kotetsu" is shown in Fig. 1. Each leg consists of three joints around the pitch axis (hip, knee

SWING

phase dynamics

initial reset: $\phi = \hat{\phi}_{PEP}$ (1)

$$\dot{\phi} = \begin{cases} \hat{\omega} + \omega_{mod} & \text{if } \phi < \hat{\phi}_{AEP} \\ 0 & \text{if } \phi = \hat{\phi}_{AEP} \end{cases} \quad (2)$$

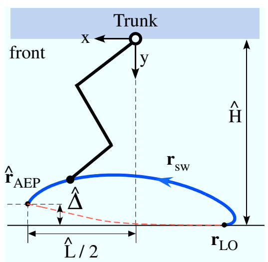

trajectory generation

$$\boldsymbol{r}_{sw}(0) = \boldsymbol{r}_{LO}$$
$$\boldsymbol{r}_{sw}(\hat{\phi}_{AEP}) = \hat{\boldsymbol{r}}_{AEP}$$
$$\begin{bmatrix} \hat{\boldsymbol{r}}_{AEP} \\ \hat{\boldsymbol{v}}_{AEP} \end{bmatrix} = \begin{bmatrix} \hat{L}/2 \\ \hat{H} - \hat{\Delta} \\ 0 \\ 0 \end{bmatrix} \quad (8)$$

TRANSITIONS

$$f_n > \hat{\chi}_{TD} \quad (3)$$
$$\& \ (\phi > \hat{\phi}_{AEP}/2) \quad (4)$$
$$f_n < \chi_{LO} \quad (5)$$

STANCE

phase dynamics

initial reset: $\phi = \hat{\phi}_{AEP}$ (6)

$$\dot{\phi} = \begin{cases} \hat{\omega} & \text{if } \phi < 2\pi \\ 0 & \text{if } \phi = 2\pi \end{cases} \quad (7)$$

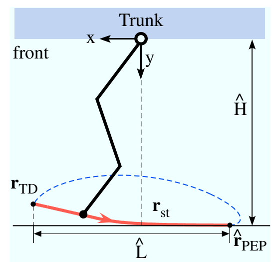

trajectory generation

$$\boldsymbol{r}_{st}(\hat{\phi}_{AEP}) = \boldsymbol{r}_{TD}$$
$$\boldsymbol{r}_{st}(2\pi) = \hat{\boldsymbol{r}}_{PEP}$$
$$\begin{bmatrix} \hat{\boldsymbol{r}}_{PEP} \\ \hat{\boldsymbol{v}}_{PEP} \end{bmatrix} = \begin{bmatrix} r_{TD,x} - \hat{L} \\ \hat{H} \\ -\hat{L}(1-\hat{\beta})/\hat{\beta}\hat{T}_{sw} \\ 0 \end{bmatrix} \quad (9)$$

$$\hat{\phi}_{PEP} = 0 \; ; \quad \hat{\phi}_{AEP} = 2\pi(1-\hat{\beta}) \quad (10) \qquad \hat{\omega} = 2\pi(1-\hat{\beta})/\hat{T}_{sw} \quad (11)$$

Fig. 2. Leg Controller structure.

and ankle) and one joint around the roll axis (hip). At the tip of each foot is a force sensor used to measured the normal ground reaction force (leg load). Kotetsu is not self-contained, and it is tethered by power and LAN cables. But the motion of Kotetsu is not affected by the cables. During dynamic walking, rolling motion in the frontal plane (with roll angle θ_{roll}) is naturally induced as a consequence of the rhythmic pitching motion of the legs because a dynamic system similar to an inverted pendulum appears in two-legged stance phases.

A gait is a locomotion pattern characterized by phase differences ($\gamma \in [0, 1]$) between the legs during their pitching motion. In the range of low- to medium-speed locomotion, medium sized mammals (like cats and dogs) mainly use the walk gait [6]. Using γ^{cntr} and γ^{ipsi} to represent respectively the phase differences between contralateral and ipsilateral legs, the walk gait is characterized by $\gamma^{cntr} = 0.5$ and $\gamma^{ipsi} \simeq 0.25$. In this study, we consider a control method to generate the walk gait in Kotetsu.

III. CPG Architecture

The phase dynamics part of the leg controller described in Section IV-A is a simple model of a CPG, the neural circuits that, in animals, generates the basic rhythmic leg motions and interleg coordination [6]. They also modulates leg phase transitions according to sensory inputs. For example, in cats, the stance-to-swing transition is prevented as long as the leg loading is over a given threshold [10]. Motivated by this fact, [8] investigated the respective importance of hip extension and leg unloading information for stance termination by 2D simulation of hind legs, and found that leg unloading plays an essential role in the emergence and stabilization of alternate stepping. In [11], leg loading was used to modulate swing and stance phases durations in a CPG control system. However, gait generation was considered at the CPG level and the contribution of phase modulations to interleg coordination and posture stabilization was not detailed.

On the other hand, we aim at achieving interleg coordination in 3D walking in an emergent fashion, through a process involving interactions with the rolling motion in the frontal plane relayed by leg loading/unloading information, rather than by explicit couplings among the leg control entities. Using such architecture, we might be able to integrate posture and rhythmic motion controls in a more sensor-dependent way in order to generate appropriate interleg coordination and give the posture control ability against lateral perturbations to some extent.

IV. Phase Modulations Based on Leg Loading/Unloading

A. Single Leg Controller

1) Overview: Our control system is based on the Central Pattern Generator (CPG) paradigm and each of the four legs is associated with a control entity that will be referred to as *leg controller* (LC), whose internal organization is schematically represented in Fig. 2 using eq.(1)∼(11). Each LC has two leg phases, *swing* (sw) and *stance* (st), and the transfer of activity between them is regulated using sensory information related to the load supported by the leg, or *leg loading/unloading*.

Each LC is associated with a simple oscillator, with a constant and unitary amplitude and a variable phase ϕ^i [1]. Such representation involving an oscillator was introduced for the sake of simplicity, to facilitate the trajectory generation process and the definition of phase relationships between the legs. However, as the phase transitions are modulated

[1]The leg index i is omitted when unambiguous. LH and RH refer to left and right hind legs, LF and RF to left and right forelegs.

using sensory feedback, sensory input has a large influence on the locomotion rhythm.

Foot trajectory generation, joint PD control and interleg coordinations as results of leg load transfer were described in detail in [7].

2) Phase dynamics: When a phase transition occurs, ϕ is reset to $\hat{\phi}_{PEP}$[2] at the swing onset (eq.(1)) or to $\hat{\phi}_{AEP}$ at the stance onset (eq.(6)). The phase then increases constantly with a rate given by the angular velocity $\hat{\omega}$, until it reaches a maximum value (as expressed by eq.(2) and eq.(7)). The parameter ω_{mod} in eq.(2) is used only by the ascending coordination mechanism (see Section IV-B) to increase the speed of the swing motion of a foreleg and is set to zero when this mechanism is inactive. Parameters $\hat{\phi}_{AEP}$, $\hat{\phi}_{PEP}$ and $\hat{\omega}$ are defined as functions of the nominal swing phase duration $\hat{T}_{sw}$ and the nominal duty ratio $\hat{\beta}$ (eq.(10) and (11)).

3) Transition conditions: The transitions between the swing and stance phases in each LC are regulated using conditions based on the normal ground reaction force f_n which is used as leg loading information. The transition from swing to stance is triggered when the contact of the foot with the ground is detected [12], [3][3], or equivalently when f_n becomes bigger than $\hat{\chi}_{TD}$ (eq.(3)).

On the other hand, the transition from stance to swing is prevented as long as the leg load is over a certain threshold (eq.(5)). The force threshold χ^i_{LO} of hind legs ($i = \{LH, RH\}$) is expressed as follows:

$$\chi^i_{LO} \quad = \quad \begin{cases} -5(N) & \text{if } \phi^i \leq \phi_{AEP} + \pi/2 \\ \hat{\chi}_{LO} & \text{otherwise} \end{cases} \tag{12}$$

where the nominal force threshold $\hat{\chi}_{LO}$ is set to a value slightly inferior to one quarter of the robot weight. χ^i_{LO} of forelegs is described in Section IV-B.

Conditions based on ϕ (eq.(4) and the upper part of eq.(12)[4]) are added just to prevent undesired early transitions, just after the transfer from one phase to the other, by leaving the time to f_n to sufficiently increase (resp. decrease) just after the touchdown (resp. the liftoff).

Stabilization of the rolling motion can be achieved by such phase modulations which consist in modulations of the respective durations of the stance and swing phases of the legs during the walking cycle. The details of this stabilization mechanism was described in [7].

B. Ascending Coordination Mechanism

In our simulation study [7], it was shown that the lateral perturbation decreasing $|\dot{\theta}_{roll}|$ caused a conflict between the control of the rhythmic pitching motions of the legs and the posture control in the frontal plane when we employed no explicit interleg coordination among LCs. Therefore, we introduced an ascending coordination mechanism (ACM) in order to solve such conflict and confirmed its effectiveness in simulations. The ACM used in simulations consisted of two parts. The first was a modulation of the foreleg force threshold χ^i_{LO}. The second was a modulation of the angular velocity of LC phase ω_{mod} of a foreleg in the swing phase.

When we implemented such twofold ACM in the control system of Kotetsu, a foreleg sometimes experienced stance-to-swing phase transition before the ipsilateral hind leg, and the gait shifted to the pace. This was caused by the asymmetric load distribution between forelegs and hind legs, since the CoM (center of mass) of the body of Kotetsu is located slightly backward from the midpoint between the hips and the shoulders. In order to solve such disorder of phase transitions, we slightly modified the ACM previously used in simulations in a way described by eq.(13), (14) and illustrated in Fig. 3.

In eq.(13), the force threshold of the foreleg χ^{sF}_{LO} (s stands for either R or L) is first linearly increased from 0 to $\hat{\chi}_{LO}$ as the phase of the ipsilateral hind leg ϕ^{sH} increases, in order to delay (or inhibit) the stance-to-swing transition of the foreleg (ACM$_{inh}$). Secondly, χ^{sF}_{LO} is linearly increased from χ^{sF}_{LO} to $\chi^{sF}_{LO} + \hat{\chi}_{ampl}$ as ϕ^{sH} increases to promote (or excite) the stance-to-swing transition of the ipsilateral foreleg (ACM$_{exc}$) and keep alternation of leg loading between contralateral legs against the lateral perturbation. Thirdly, the stance-to-swing transition of the foreleg is inhibited during the stance phase of the ipsilateral hind leg. The first and third parts are newly employed for experiments using Kotetsu in order to prevent the disorder of the phase transitions described above. The second is exactly same with the one used in simulations [7].

$$\chi^{sF}_{LO} \quad = \quad \begin{cases} \tau_{acm} \cdot \hat{\chi}_{LO} & \text{if } \phi^{sH} < \hat{\phi}_{acm} \\ \hat{\chi}_{LO} + \chi_{mod} & \text{if } \phi^{sH} \in [\hat{\phi}_{acm}; \hat{\phi}_{AEP}] \\ -5(N) & \text{if } \phi^{sH} > \hat{\phi}_{AEP} \end{cases} \tag{13}$$

$$\chi_{mod} = \tau_{mod}(\phi^{sH}) \cdot \hat{\chi}_{ampl}$$

where $\hat{\phi}_{acm} = 0.5 \cdot \hat{\phi}_{AEP}$, $\tau_{acm} = \phi^{sH}/\hat{\phi}_{acm}$ and

$$\tau_{mod}(\phi) = (\phi - \hat{\phi}_{acm})/(\hat{\phi}_{AEP} - \hat{\phi}_{acm}).$$

In eq.(14), ϕ^{sH}_{LO} is the LC phase of the hind leg at the moment when the foreleg transits to the swing phase. If ϕ^{sH}_{LO} is greater than $\hat{\phi}_{acm}$, it means that the transition to the swing phase of the foreleg is delayed. Therefore, we make the swing motion of the foreleg faster in order to compensate such delay of the transition (ACM$_\omega$). This ACM$_\omega$ is identical to the one used in simulations. It contributes to reduce the increase of the amplitude of the roll angle of the body by shortening the duration of the swing phase of the foreleg just after a lateral perturbation [7].

$$\omega^{sF} = \hat{\omega} + \omega^{sF}_{mod} \tag{14}$$

$$\omega^{sF}_{mod} = \begin{cases} 0.5 \cdot \tau_{mod}(\phi^{sH}_{LO}) \cdot \hat{\omega} & \text{if } \phi^{sH}_{LO} \in [\hat{\phi}_{acm}; \hat{\phi}_{AEP}] \\ 0 & \text{otherwise} \end{cases}$$

[2]The hat symbol ˆ is used in this paper to represent the nominal value of a variable.

[3]They reported that such phase resetting modulated the gait and enhanced the stability against perturbations.

[4]The value -5 is not important and it works as far as the value is negative.

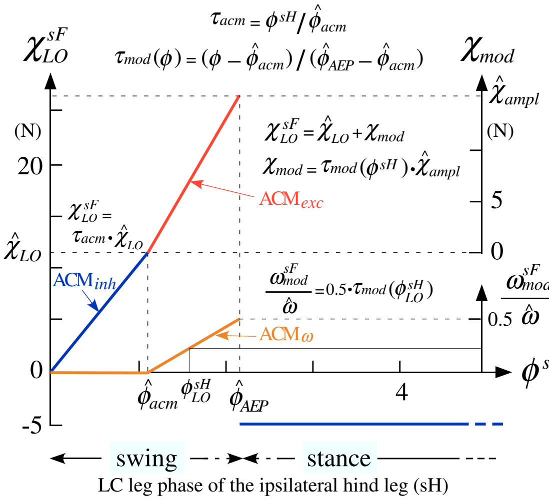

Fig. 3. The twofold ACM employed in the control system of Kotetsu. Modulations of force threshold χ_{LO}^{sF} in the stance phase and angular velocity of LC phase ω_{mod}^{sF} in the swing phase of a foreleg (sF) are shown as functions of the LC phase ϕ^{sH} of the ipsilateral hind leg (sH).

V. Experiments with Lateral Perturbation

In [9], we reported the realization with Kotetsu of a walk gait characterized by a cyclic period T=0.64s, β=0.71, γ^{ipsi}=0.21, and a walking speed V=0.2m/s. We use here a similar gait with long cyclic period, for which posture control in the frontal plane is particularly challenging.

In order to apply a lateral perturbation, we hung a pendulum consisting of a mass (0.2kg) and a string (0.35m). Kotetsu was struck at the center of the body (Fig. 1) from the left to the right by the mass after releasing the pendulum at an angle of 90 deg. to the vertical axis (elastic collision, an impulse of approx. 0.56 Kgm/s).

The experimental results are shown in Fig. 4, 5 and 6. In all figures, ground contact, LC phase, leg load f_n^i with force threshold of a foreleg χ_{LO}^{sF} and body roll angle are shown. Parameter settings used in experiments are shown in Table I. Since ACM$_{inh}$ was used in all experiments, we can see that χ_{LO}^{sF} was linearly increased from 0 to $\hat{\chi}_{LO}$ as the phase of the ipsilateral hind leg ϕ^{sH} increased. In the experiments without ACM$_{exc}$ and ACM$_{\omega}$, χ_{mod} and ω_{mod}^{sF} were 0 in eq.(13) and eq.(14), respectively. While calculating eq.(13), the value of χ_{LO}^{sF} was fixed temporarily when eq.(5) was satisfied and the stance-to-swing phase transition of the foreleg was triggered, in order for readers to easily understand its value. Afterwards, the value of χ_{LO}^{sF} was set to -5 by the third of eq.(13). After a stance-to-swing phase transition in the LC, the leg needs time to unload. This explains the delay of approx. $0.03s$ between LC transition and liftoff event (clearance of ground contact).

In Fig. 4, a lateral perturbation was applied at timing where all legs were in the stance phase and it caused $|\dot{\theta}_{roll}|$ to increase, leading to a temporary augmentation of rolling motion amplitude. As a consequence, the lateral transfer of leg loading was accelerated. The additional load supported by the right legs caused their stance phase to be prolonged (A and B), while the swing phase of the left legs to be prolonged (C and D). As a result, rolling motion was stabilized by the mechanism described in [7] without ACM$_{exc}$ and ACM$_{\omega}$.

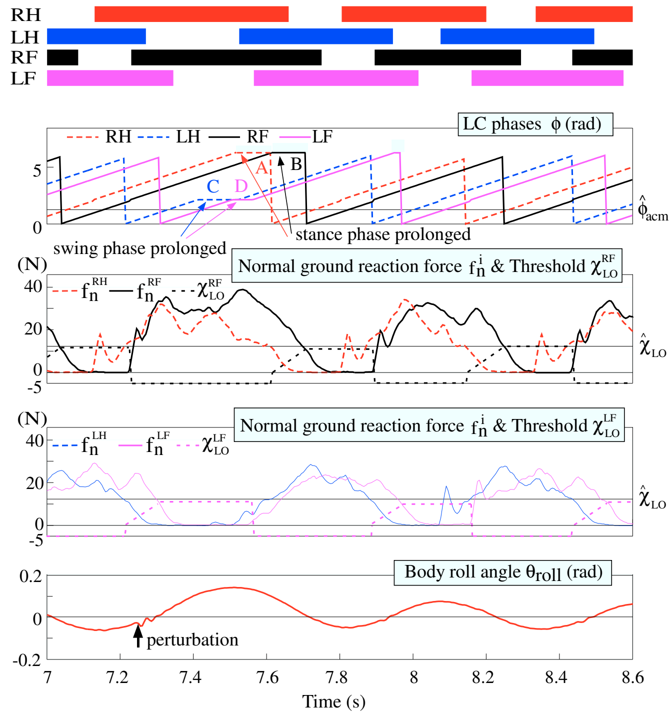

Fig. 4. Results of an experiment against the lateral perturbation increasing $|\dot{\theta}_{roll}|$ without ACM$_{exc}$ and ACM$_{\omega}$.

In Fig. 5 and Fig. 6, a lateral perturbation was applied at timing where left fore and hind legs were in the swing phase and $|\dot{\theta}_{roll}|$ decreased. If the stance-to-swing phase transition was not triggered while χ_{LO}^{sF} was increased by ACM$_{inh}$, χ_{LO}^{sF} in Fig. 5 was kept constant afterwards since ACM$_{exc}$ was not employed. On the other hand, χ_{LO}^{sF} in Fig. 6 was consequently linearly increased by ACM$_{exc}$ until the condition for stance-to-swing transition was satisfied $(f_n^{sF} < \chi_{LO}^{sF})$.

In Fig. 5, decreasing $|\dot{\theta}_{roll}|$ led to a temporary diminution of the rolling motion amplitude. This tended to cancel the rolling motion and the associated lateral transfer of leg loading. Accordingly, the rate of unloading of RF decreased and, f_n^{RF} did not become smaller than the threshold χ_{LO}^{RF} which was not increased by ACM$_{exc}$. The transition to the swing phase of the LC of RF was prevented, which greatly disturbed the interleg coordination. In the case of Fig. 5, since the stance-to-swing transition of RF was durably prevented, the stance-to-swing transition of LF was also

Parameter settings					
$\hat{H}$	(m)	0.22	$\hat{L}$	(m)	0.04
$\hat{\chi}_{LO}$	(N)	12	$\hat{\chi}_{TD}$	(N)	2
$\hat{T}_{sw}$	(s)	0.2	$\hat{\beta}$		0.66
$\hat{\Delta}^{*F}$	(m)	0.01	$\hat{\Delta}^{*H}$	(m)	0
$\hat{\chi}_{ampl}$	(N)	15			

TABLE I

Parameter settings for experiments shown in Fig. 4, 5 & 6.

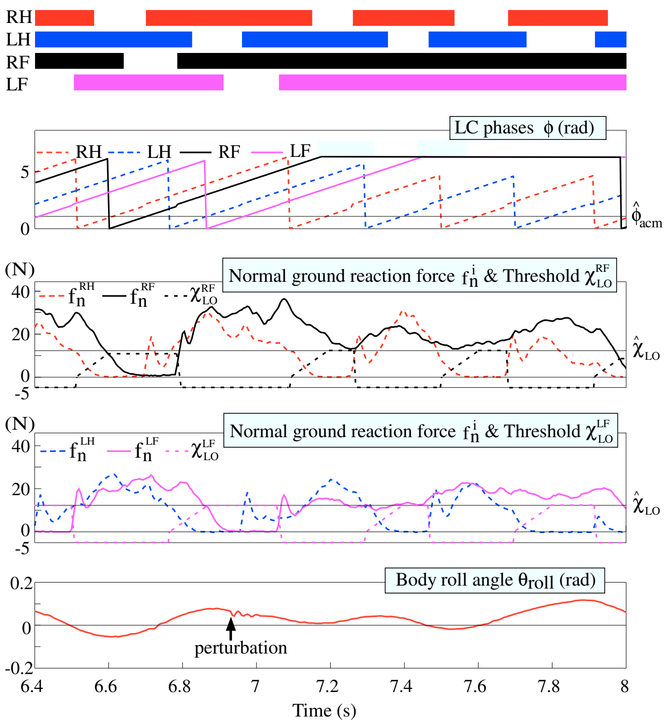

Fig. 5. Results of an experiment against the lateral perturbation decreasing $|\dot{\theta}_{roll}|$ without ACM$_{exc}$ and ACM$_{\omega}$.

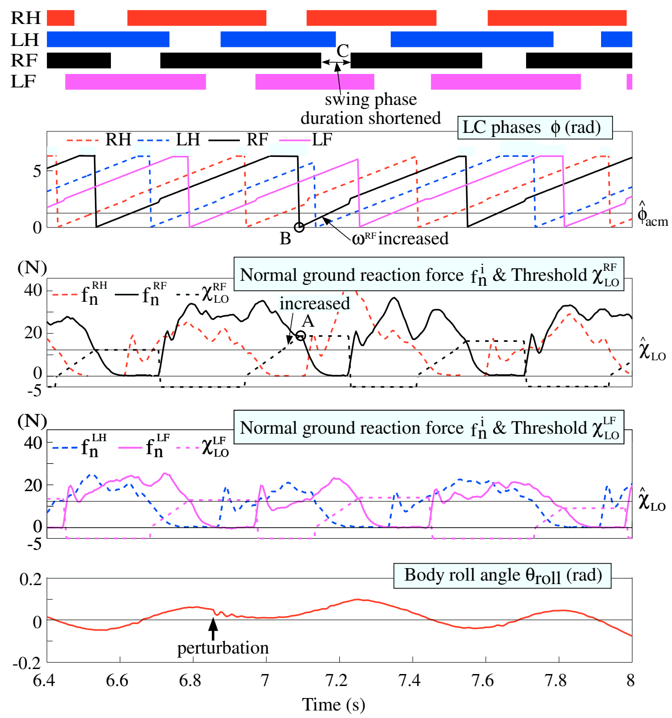

Fig. 6. Results of an experiment against the lateral perturbation decreasing $|\dot{\theta}_{roll}|$ with ACM$_{exc}$ and ACM$_{\omega}$.

durably prevented. Consequently Kotetsu fell forward.

In Fig. 6, the rate of unloading of RF decreased after a lateral perturbation, and f_n^{RF} was still larger than $\hat{\chi}_{LO}$. But as χ_{LO}^{RF} was increased by ACM$_{exc}$, eq.(5) was satisfied (◯ A) and the stance-to-swing transition of the LC of RF was triggered (◯ B). In addition, we can see in Fig. 6 that ω^{RF} in the swing phase of RF was increased and the swing phase duration of RF was shortened (↔ C) by ACM$_{\omega}$. Consequently, the order of phase transitions characteristic of a walk gait was preserved, the rolling motion was stabilized, and Kotetsu kept walking successfully.

Snapshots of a successful experiment with ACM$_{exc}$ and ACM$_{\omega}$ are shown in Fig. 7. We can see that the foot tip of RF was on the floor just after impact (b) and lifted off at approx. 0.3s after impact (c) as the result of the stance-to-swing phase transition of the LC of RF caused by ACM$_{exc}$. In addition, since ω^{RF} was increased and the swing phase duration of RF was shortened by ACM$_{\omega}$, the foot tip was able to reach $\hat{\boldsymbol{r}}_{AEP}$ (Fig. 2) before landing on the floor as shown in (d). Hence, th stumbling of RF was avoided. Afterwards, correct phase transitions (e) and (f) followed.

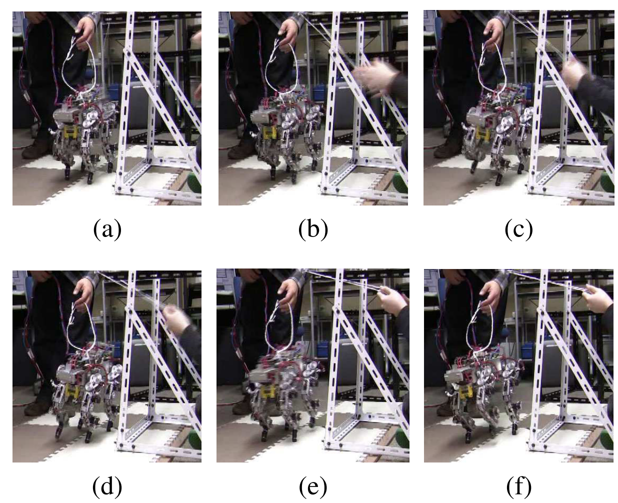

Fig. 7. Snapshots of a lateral perturbation experiment with ACM$_{exc}$ and ACM$_{\omega}$ (T=0.74s and V=0.1m/s). (a) at impact. (b) and (c) just and 0.3s after impact. (d), (e) and (f) afterwards. These snapshots are not exactly corresponding to Fig. 6.

VI. Discussions

A. Comparison with simulations

Summary of conditions of a perturbation and each ACM in simulations and experiments, and comparisons of both results are shown in Table II. In order to represent the timing of a lateral perturbation, we use ↑ and ↓, which mean that $|\dot{\theta}_{roll}|$ is temporary increased and decreased after the perturbation, respectively. The figure numbers in our simulation study paper[7] (in *italic*) and in this paper are also shown. The marks × and ∘ mean that each ACM is not employed, or employed. The result: "success", "fail" or "disorder" mean that a quadruped kept walking, fell or showed disordered phase transitions, respectively.

In simulations, it was shown that the method using phase modulations based on leg unloading had the ability to stabilize posture against perturbations increasing $|\dot{\theta}_{roll}|$ (↑) without explicit interleg coordinations by the stabilization mechanism described in [7]. But we needed the twofold ACM (ACM$_{exc}$ and ACM$_{\omega}$) to withstand perturbations de-

	perturbation	ACM_{inh}	ACM_{exc}	ACM_{ω}	result
sim.	no (*Fig.6*)	×	×	×	success
sim.	↑ (*Fig.12*)	×	×	×	success
sim.	↓ (*Fig.13*)	×	×	×	fail
sim.	↓ (*Fig.14*)	×	◦	◦	success
exp.	no	×	×	×	disorder
exp.	no	◦	×	×	success
exp.	↑ (Fig. 4)	◦	×	×	success
exp.	↓ (Fig. 5)	◦	×	×	fail
exp.	↓ (Fig. 6)	◦	◦	◦	success

TABLE II

SUMMARY OF CONDITIONS OF A PERTURBATION AND EACH ACM IN SIMULATIONS AND EXPERIMENTS, AND COMPARISONS OF RESULTS.

creasing $|\dot{\theta}_{roll}|$ (↓).

In experiments, we always needed ACM_{inh} not for stabilizing posture, but for preventing the disorder of the phase transitions due to the backward position of CoM. For perturbations decreasing $|\dot{\theta}_{roll}|$ (↓) (resp increasing $|\dot{\theta}_{roll}|$ (↑)), we did (resp. did not) need ACM_{exc}. These observations match our previous simulation results, when the robot is subjected to lateral perturbations [7].

B. Effectiveness of the ACM

The experimental result shown in Fig. 5 also confirms that an additional mechanism is needed to help the system to recover when the rolling motion amplitude is suddenly reduced. The situation that occurs in that case can be seen as a conflict between the control of the rhythmic pitching motions of the legs, which requires the stance-to-swing phase transition of the foreleg to preserve the coordination, and the posture control in the frontal plane, which prevents it because a leg still supporting the body should not swing to preserve the balance. For that reason, the ACM (ACM_{exc} and ACM_{ω}) described in Section IV-B was introduced at that point. While allowing the foreleg to swing, the ACM globally increases the duty ratio of the foreleg: the transition to the swing phase is still delayed compared to normal (hence the stance phase is extended) while the next swing phase duration is shortened. Moreover, the increase of the duty ratio is positively related with the increase of the load supported by the foreleg (i.e. with the intensity of the perturbation). Consequently, the ACM works in cooperation with the stabilization provided by the phase modulations as shown in Fig. 6. Moreover, ACM_{ω} has a role to prevent a foreleg from the stumbling in a swing phase and to help it land on the correct forward position as show in Fig. 7.

C. Increasing the intensity of lateral perturbations

Obviously, the method proposed in this study can not stabilize walking, when we increase the intensity of lateral perturbations[5]. As we described in [7], [9], we will have to employ sideway touchdown angle control (a stepping reflex) based on rolling motion information [4], [5], [13] to cope with large intensity of lateral perturbations and terrains of medium degrees of irregularity. But in order to show the basis of a general legged locomotion controller, we are now investigating the meaning of phase modulations based on leg loading/unloading and so on while being combined with minimum interleg coordinations referring to biological knowledge. We expect that such method is a fundamental mechanism, contributing to posture control, and that it would give redundant and robust functions when adding a stepping reflex in future.

[5]The maximum intensity of lateral perturbations without falling was investigated in simulations[7].

VII. CONCLUSIONS

In our previous simulation study, rhythmic motion control including interleg coordinations and its integration with posture control were achieved while utilizing the body dynamics and the characteristics of legged locomotion under a gravity field. In this study, we confirmed the validity of those simulations by experiments, even though we used a slightly modified ascending coordination mechanism (ACM) to cope with disturbances by the backward position of CoM in Kotetsu. Our control system, relying on phase modulations based on leg loading/unloading and the ACM between ipsilateral legs, enabled stable walking against lateral perturbations.

REFERENCES

[1] Takanishi, A., Takeya, T., Karaki, H. & Kato, I. (1990). A control method for dynamic biped walking under unknown external force. In *Proc. of IROS 1990*, 795-801.

[2] Yoneda, K., Iiyama, H. & Hirose, S. (1994). Sky-hook suspension control of a quadruped walking vehicle. In *Proc. of ICRA 1994*, 999-1004.

[3] Aoi, S. & Tsuchiya, K. (2006). Stability analysis of a simple walking model driven by an oscillator with a phase reset using sensory feedback. *IEEE trans. on Robotics* 22(2), 391-397.

[4] Fukuoka, Y., Kimura, H. & Cohen, A. (2003). Adaptive dynamic walking of a quadruped robot on irregular terrain based on biological concepts. *I. J. of Robotics Res.*, 22(3-4), 187-202.

[5] Kimura, H., Fukuoka, Y. & Cohen, A. H. (2007). Adaptive dynamic walking of a quadruped robot on natural ground based on biological concepts. *I. J. of Robotics Res.*, 26(5), 475-490.

[6] Orlovsky, G. N., Deliagina, T. G., & Grillner, S. (1999). *Neural control of locomotion*. Oxford Univ. Press, New York.

[7] Maufroy, C., Kimura, H. & Takase, K. (2010). Integration of posture and rhythmic motion controls in quadrupedal dynamic walking using phase modulations based on leg loading/unloading, *Autonomous Robots* 28(3), 331-353.

[8] Ekeberg, O. & Pearson, K. (2005). Computer simulation of stepping in the hind legs of the cat: an examination of mechanisms regulating the stance-to-swing transition. *J. of Neurophysiology*, 94(6), 4256-68.

[9] Maufroy, C., Nishikawa, T. & Kimura, H. (2010). Stable dynamic walking of a quadruped robot "Kotetsu" using phase modulations based on leg loading/unloading. *Proc. of ICRA 2010*, 5225-5230.

[10] Duysens, J. & Pearson, K.G. (1980). Inhibition of flexor burst generation by loading ankle extensor muscles in walking cats. *Brain Res.*, 187, 321-32.

[11] Righetti, L. & Ijspeert, A. (2008). Pattern generators with sensory feedback for the control of quadruped locomotion. In *Proc. of ICRA 2008*, 819-824.

[12] Tsujita, K., Tsuchiya, K. & Onat, A. (2001). Adaptive gait pattern control of a quadruped locomotion Robot. In *Proc. of IROS2001*, 2318-2325.

[13] Boston Dynamics (2005). BigDog project. http://www.bdi.com/content/sec.php?section=BigDog